BULLETIN OF THE POLISH ACADEMY OF SCIENCES
TECHNICAL SCIENCES, Vol. 60, No. 3, 2012
DOI: 10.2478/v10175-012-0070-1

SAW sensor for detection of hydrocarbons. Numerical analysis and experimental results

T. HEJCZYK[1], M. URBAŃCZYK[2*], R. WITUŁA[3], and E. MACIAK[2]

[1] ENTE Ltd, limited liability company, 7 Gaudiego St., 44-100 Gliwice, Poland
[2] Faculty of Electrical Engineering, Silesian University of Technology, 2 Krzywoustego St., 44-100 Gliwice, Poland
[3] Faculty of Applied Mathematics, Silesian University of Technology, 2 Kaszubska St., 44-100 Gliwice, Poland

Abstract. The paper presents the results of numerical analyses of the SAW gas sensor in the steady and non-steady state. The effect of SAW velocity changes vs. the surface electrical conductivity of the sensing layer is predicted. The conductivity of the porous sensing layer above the piezoelectric waveguide depends on the profile of the diffused gas molecule concentration inside the layer. Knudsen's model of gas diffusion was used. Numerical results for the gases CH_4, C_2H_4, C_3H_8, C_6H_6 in the steady state and CH_4 in the non-steady state in the WO_3 sensing layer have been shown. The results of numerical analyzes allow to select the sensor design conditions, including the morphology of the sensor layer, its thickness and operating temperature. Some numerical results were verified in experimental studies concerning methane.

Key words: SAW, gas sensor, piezoelectric substrate, Ingebrigtsen's formula, impedance transformation law, numerical modeling.

1. Introduction

There is currently a great need for monitoring the concentration of explosive gases. At very low concentrations of these gases they are usually preconcentrated to obtain a low detection limit. Various methods have been developed to detect these gases [1, 2]. The sensor using the propagation of Rayleigh surface acoustic waves (SAW) containing a suitably chosen chemically sensitive layer is adequate for detecting low concentrations of gases. For this purpose on a piezoelectric substrate (e.g. $LiNbO_3$) two identical acoustic delay lines are performed. They work in the feedback loop of the amplifiers forming two oscillators. The acoustic surface wave is excited by interdigital transducers. On one line a thin sensing layer of the semiconductor, e.g. WO_3, with a catalytic layer is formed by means of the PVD method [3, 4]. The free path serves as a reference one, permitting easy measurements of the resulting difference in the frequency of the two oscillators. The output sensor signal is a signal with a frequency that depends on the gas concentration in the environment. Diffusion of gas molecules into the sensor layer changesw its physical properties, especially the electrical conductivity. This effect causes a change in boundary conditions for wave propagation. There is a change in wave attenuation, and a change in the velocity of propagation. This phenomenon is used in an acoustic gas sensor. It is a well-known acoustoelectric phenomenon [5–7]. The main advantage of using surface waves in the sensor is that the wave energy is concentrated in a thin layer of the waveguide (not exceeding 2 λ). This provides a strong coupling of the wave with the sensor layer by the electric field of the mechanical wave in piezoelectric substrate.

Changes in electrical properties of sensor layers depend on the concentration of gas molecules in the volume and also on the size of the gas molecules, the layer morphology, porosity and thickness, and the temperature of the layer. Numerical analysis of the impact of these parameters on the sensor response is important for the proper construction of the sensor. This analysis can be performed basing on the developed analytical model of a SAW sensor.

2. Analytical model of a gas sensor

In order to optimize the structure of the sensor it is important to get an analytical model of the SAW sensor. The intensity interaction of the electric field with a sensing layer in a surface wave sensor depends not only on the electrical conductivity of the layer, but also on its distance from the piezoelectric waveguide. More details about the analytical model can be found in the paper by Hejczyk and Urbańczyk [4–9]. Analyzing the acoustoelectric effect in a SAW sensor, the sensing layer was assumed to consist of n-thin sublayers (Fig. 1), in which the concentration of the diffused gas molecules differs, but is constant in the respective sublayer [5].

The assumption that the electrical conductivity of the respective layers $\sigma(y)$ is proportional to the concentration of the gas molecules C_A in these sublayers is of essential importance:

$$\sigma(y) = \sigma_0 \left(1 + a\, C_A(y)\right), \tag{1}$$

where σ_0 and a are the conductance of the upper layer and sensitivity parameter, respectively.

In order to obtain an analytical model of a SAW gas sensor, we must find the equivalent electrical impedance on the surface of the piezoelectric waveguide. For this purpose, we apply the law of transformation of the impedance. The impedance of the sublayer at a given distance from the surface of the piezoelectric waveguide is transformed to this surface

*e-mail: Marian.Urbanczyk@polsl.pl

($y = 0$). Figure 2 shows a schematic diagram of the action of the impedance transformation law. Using the transformation law for the n-th sublayer, it is possible to calculate the electrical admittance on the surface of the waveguide, which is "seen" by the surface wave. Then, the resultant of the admittance is used in Ingebrigtsen's formula [9–11] to determine the changes in the velocity of the surface wave resulting from the acoustoelectric interaction between the SAW and the sensor layer with a variable concentration of gas molecules in the y direction (in the depth of the layer).

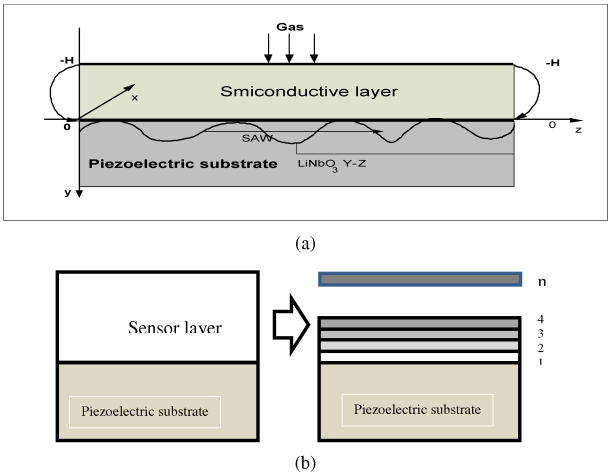

Fig. 1. Exemplary model (a) and equivalent model (b) of the analyzed multilayer sensor structure after Ref. [5]

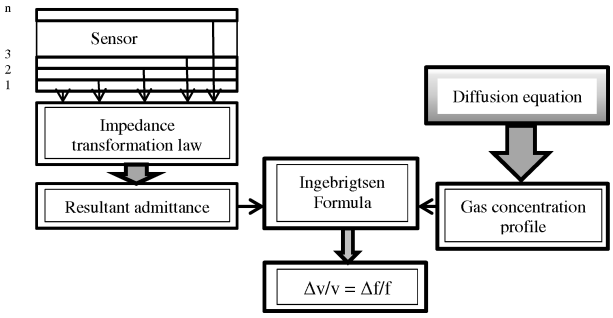

Fig. 2. Analytical diagram of a SAW gas sensor after Ref. [5, 9]

It can be shown, that the Ingebrigtsen formula for n-sublayers takes the following form [5, 9]:

$$\frac{\Delta v}{v_0} = -Re\left\{\frac{\Delta k}{k_0}\right\} = -\frac{K^2}{2} \cdot \frac{\left[\sigma_{T_2}(1 + aC_{A,y=0}) + \sum_{i=1}^{n-1} \sigma_{T_2}(y_i) f(y_i, \sigma_{T_2}(y_i))\right]^2}{ZZ}, \quad (2)$$

where

$$ZZ = \left[\sigma_{T_2}(1 + aC_{A,y=0}) + \sum_{i=1}^{n-1} \sigma_{T_2}(y_i) f(y_i, \sigma_{T_2}(y_i))\right]^2 + \left[1 + \sum_{i=1}^{n-1} g(y_i, \sigma_{T_2}(y_i))\right]^2 (v_0 C_S)^2,$$

n – number of sublayers and $C_S = \varepsilon_0 + \varepsilon_p^T$,

$$\sigma_{T_2} = \sigma_{T_1} \exp\left(\frac{E_g}{2k_B} \cdot \frac{T_2 - T_1}{T_1 T_2}\right),$$

$$T_1 = 300 \text{ K}, \qquad \sigma_{T_1} = \sigma_0,$$

k_B – Boltzman constant, E_g – band gap energy, ε_o and ε_p^T are respectively, dielectric permittivity of the vacuum and piezoelectric substrate (upper subscript T means in constant stress condition),

$$f(y_i, \sigma_s) = \frac{1 - [\text{tgh}(ky_i)]^2}{[1 + \text{tgh}(ky_i)]^2 + \left[\text{tgh}(ky_i) \cdot \frac{\sigma_s}{\varepsilon_0 v_0}\right]^2},$$

$$g(y_i, \sigma_s) = \frac{[1 + \text{tgh}(ky_i)]^2 + \text{tgh}(ky_i) \cdot \left(\frac{\sigma_s}{\varepsilon_0 v_0}\right)^2}{[1 + \text{tgh}(ky_i)]^2 + \left[\text{tgh}(ky_i) \cdot \frac{\sigma_s}{\varepsilon_0 v_0}\right]^2}$$

and $\sigma(y_i) = \sigma_0[1 + a \cdot C_A(y_i)]$, v_o – SAW velocity, k – wave number ($k = 2\pi/\lambda$).

In this analysis it has been assumed that the diffusion of the gas molecules into the sensing layer is of the Knudsen type, which occurring in the pores with diameters of 1 to 100 nm. In such a case the average free path of the diffusing particles is restricted by colliding with the walls of the pores, and not by their collisions with other particles. The concentration profile decreases monotonically with the depth of the layer. We also assume that we have to do with a chemical reaction of the first order in the sensor layer. It means that its speed is proportional to the concentration of only one reagent. The equation of the diffusion may be expressed as follows [14, 15]:

$$\frac{\partial C_A(y,t)}{\partial t} = D_K \frac{\partial^2 C_A(y,t)}{\partial y^2} - kC_A(y,t), \quad (3)$$

where $C_A(y,t)$ – concentration of gas molecules at the distance y from the upper surface of the sensor layer at the moment t (Fig. 1a), D_K – constant of the Knudsen diffusion, k – reverse reaction rate constant in a layer that describes the reduction in the concentration of gas molecules in the layer.

The profile of the concentration in the steady-state (Fig. 3), resulting from the solution of the one-dimensional equation of diffusion takes the following form:

$$C_A = C_{A,S} \frac{\cosh(|y| \sqrt{k/D_k})}{\cosh(|-H| \sqrt{k/D_k})}, \quad (4)$$

where $C_{A,s}$ denotes the concentration of gas on the top surface of the sensor layer.

Figure 3 shows an exemplary steady-state profile the concentration of gas molecules in a sensor layer with a thickness of 300 nm and for $k/D_K = 10^{-4}$ nm^{-2}.

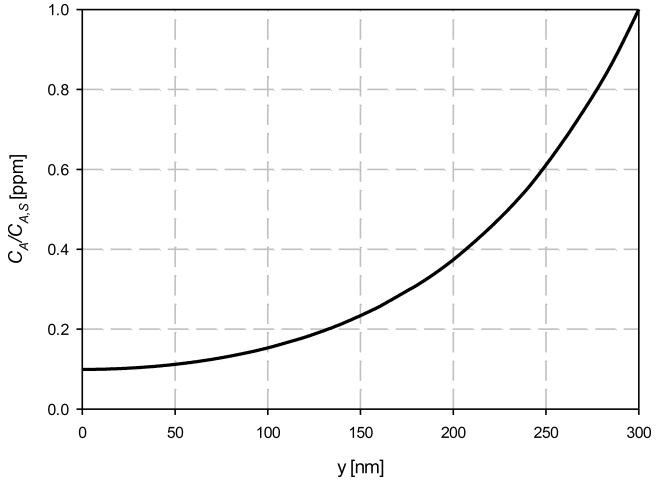

Fig. 3. Profile of the gas concentration in the layer with a thickness of $H = 300$ nm

The gas diffusion equation in the transient state can be solved using the Fourier transform [12]. The solution is of the form [13, 14]:

$$C_A(y,t) = C_{A,S}\left[1 - \frac{2}{\pi}\sum_{n=1}^{\infty}\frac{1-(-1)^n}{n}\left[\exp(-\omega_n^2 t) + \frac{k\left(1-(1+\omega_n^2 t)\exp(-\omega_n^2 t)\right)}{\omega_n^2 + k(1-\exp(-\omega_n^2 t))}\right]\sin\frac{n\pi(H-y)}{2H}\right], \tag{5}$$

where $\omega_n = \frac{n\pi\sqrt{D_K}}{2H}$, $C_{A,S}$- concentration on the top surface of the sensor layer, n – number of iterations, H – thickness of the semiconducting sensor layer.

The solution quoted above allows to analyze changes in the concentration-time profile of the distribution of gas molecules. Applying this solution in the analytical model of the SAW sensor [5, 9], we can analyze the dynamics of the sensor response in transient state.

Figure 4 shows the time dependence of the gas concentration profiles (concerning the time from $t = 10^{-9}$ to 10^{-7} sec). Diffusion model allows to analyze the gas concentration profiles in the sensor layer depending on the rate constant k (Fig. 5), and the value of Knudsen's diffusion constant (D_K) (Fig. 6).

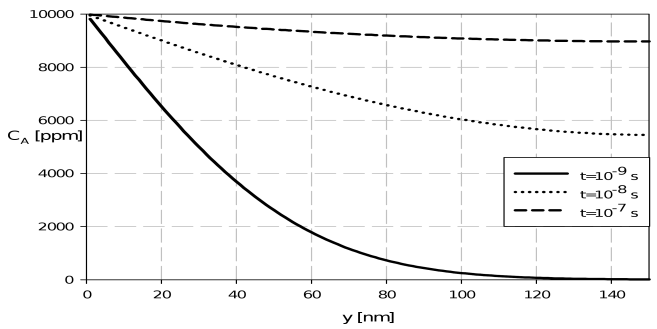

Fig. 4. Concentration profiles for gas vs. the layer thickness in the moments $t = 10^{-9}, 10^{-8}, 10^{-7}$ ns, for $C_{A,s} = 10000$ ppm, $n = 10$, k= 10^7 s^{-1}, $D_K = 10^8$ nm^{2}s^{-1}

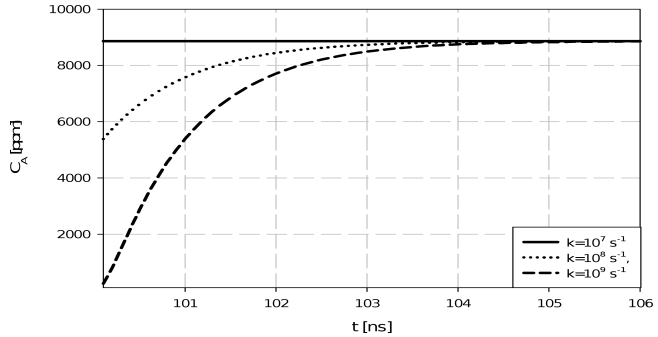

Fig. 5. The gas concentration profiles versus time at different rate constants $k = 10^7$ s^{-1}, $k = 10^8$ s^{-1}, $k = 10^9$ s^{-1} and for $C_{A,s} = 10000$ ppm, $n = 10$, $D_K = 10^{12}$ nm^{2}s^{-1}

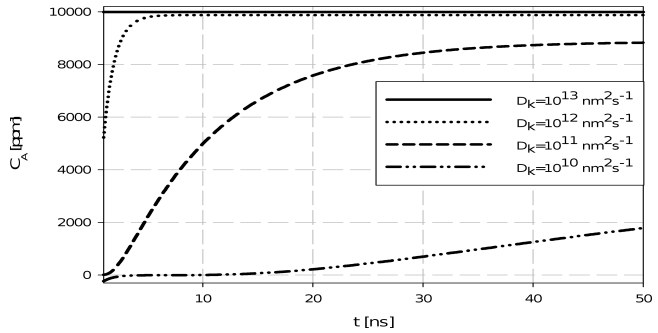

Fig. 6. The gas concentration profiles versus time at different values of diffusion coefficient $D_K = 10^{13}$ nm^{2}s^{-1}, 10^{12} nm^{2}s^{-1}, 10^{11} nm^{2}s^{-1}, 10^{10} nm^{2}s^{-1} and for $k = 10^8$ s^{-1}, $C_{A,s} = 10000$ ppm, $n = 10$

3. Numerical analysis of the acoustoelectric interaction in the sensing layer

An acoustoelectric interaction of surface waves with charge carriers in the layer of the sensor, which are formed by the diffusion of the hydrocarbon molecules CnHn was analyzed numerically in the Payton software, both in the steady and transient state. Sensor responses are shown in Figs. 7 and 8. The following diagrams show the results of the analysis of sensor response depending on the type of gases (Fig. 7a), pore radius Fig. 7b) and the thickness of the sensing layer (Fig. 7c) as well as operating temperature of the sensor (Fig. 7d) (relative changes in wave propagation velocity with respect to the parameters given above). The numerical analysis concerns the semiconductor layer WO_3 with an energy gap $E_g = 2.7$ eV.

Figure 7c shows that there is an optimal thickness of the sensor layer (30–40 nm), for which the acoustoelectric effect is greatest (minimum on the graph) in the case of all hydrocarbon molecules. Furthermore, the optimal operating temperature of the sensor is slightly higher than 340 K (Fig. 7d).

The analysis of the transition state, shown in Fig. 8, allows to observe temporal changes in the response of the sensor. The response of the WO_3 semiconductor layer on the methane CH_4 in the transition state was analyzed in the time from $t = 10^{-12}$ sec to $t = 10^{-3}$ sec, depending on the gas concentration (Fig. 8a), the dimensions of the radius of the pores (Fig. 8b), the layer thickness (Fig. 8c) and temperature (Fig. 8d).

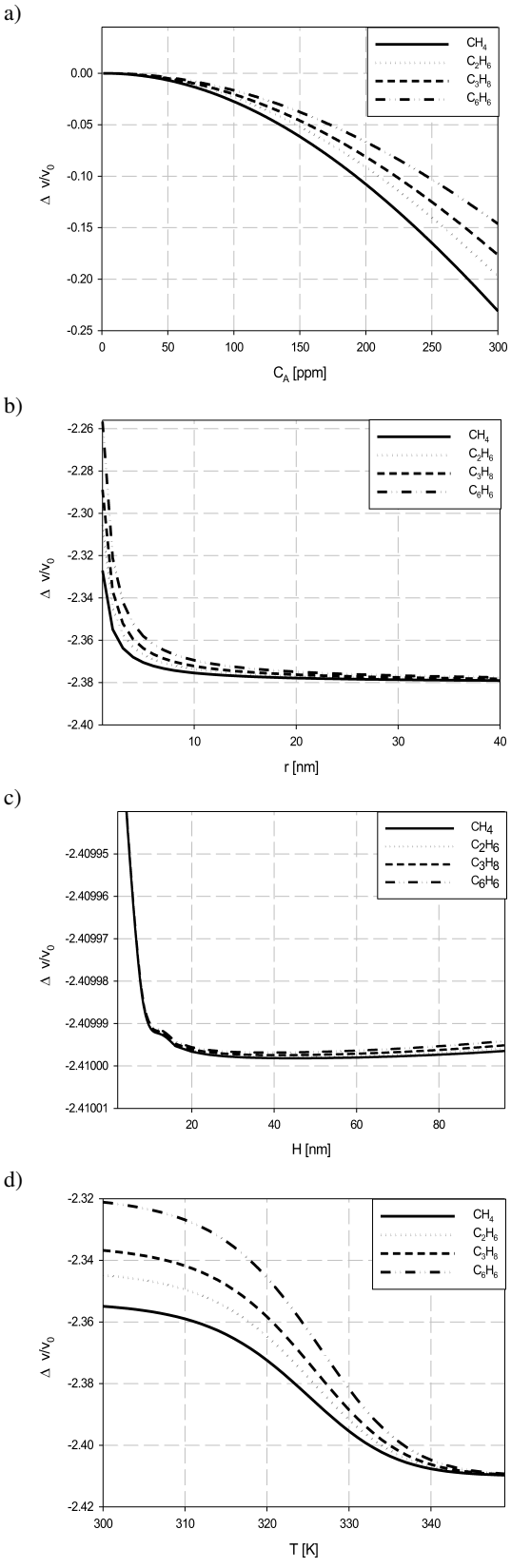

Fig. 7. **SAW** wave velocity changes vs.: a) concentration of CH_4, C_2H_4, C_3H_8, C_6H_6, b) pore radius, c) temperature and d) sensing layer thickness. The results are presented assuming the following values have become involved $\sigma_s = v_0 C_S = 4.7 \cdot 10^{-8}\ \Omega^{-1}$, sensitivity coefficient $a = 1$ ppm^{-1}, thickness of the sensor layer 100 nm, temperature 371 K, pore radius 2 nm, WO_3 layer ($E_g = 2.7$ eV)

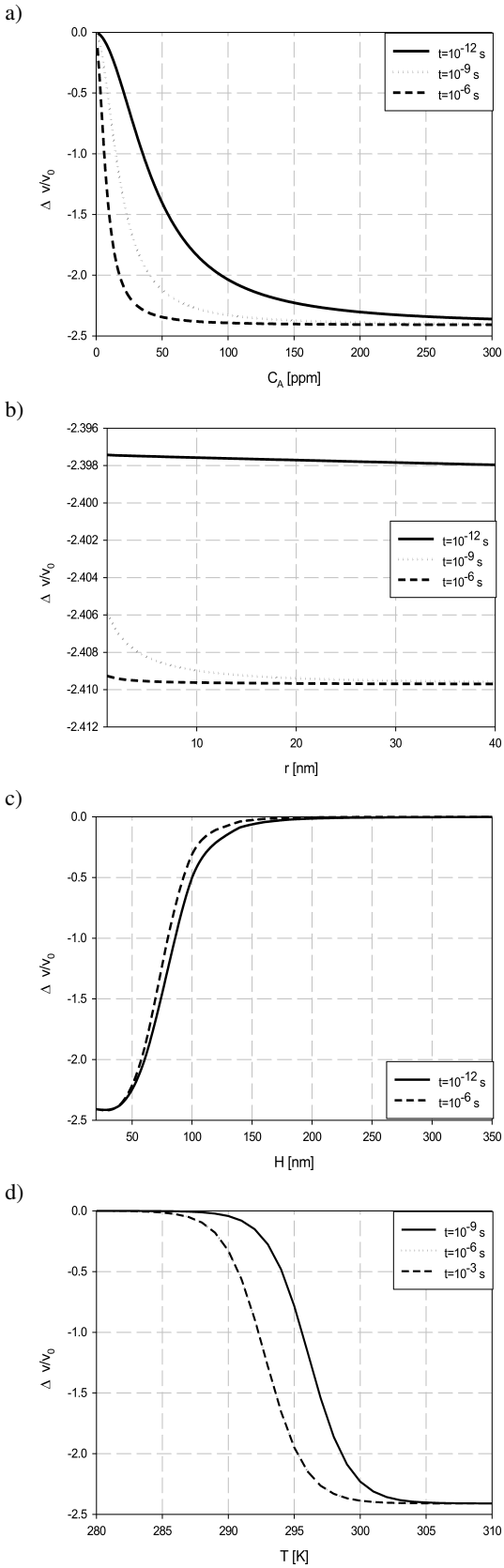

Fig. 8. SAW wave velocity changes in transient state vs.: a) gas concentration of CH_4, b) layer thickness, c) pore radius and d) temperature at times $t = 10^{-12}$ to 10^{-3} sec for $k = 10^{12}$ s^{-1}, $D = 10^{12}$ nm^{2}s^{-1}, WO_3 layer ($E_g = 2.7$ eV)

4. Experimental results

Experimental studies were performed on a sensor with three layers of WO_3 + Pd. The sensor layer thicknesses were, respectively, 50 nm + 10 nm, 100 nm + 10 nm and 150 nm + 10 nm. The study was performed in methane. Sensor layers were deposited using the PVD method on a piezoelectric plate of lithium niobate $LiNbO_3$ – YZ cut with dimensions $20 \times 30 \times 0.5$ mm. Vacuum PVD techniques allow to obtain layers with the thicknesses from a few to several hundred nanometers, covering a wide range of materials. Layers of tungsten oxide WO_3 were prepared by vacuum evaporation at a pressure of $1 \cdot 10^{-3}$ Pa. The WO_3 vapor source was a powder with a purity of 99.9% (Aldrich). The sublimation temperature of the molybdenum heater was 1100 ± 100°C. The mean tungsten oxide deposition rate under these conditions was 1.5 nm/sec. The lithium niobate substrate on which the layers were deposited, was not heated during the deposition process. In this way layers of amorphous tungsten oxide were obtained (Fig. 9).

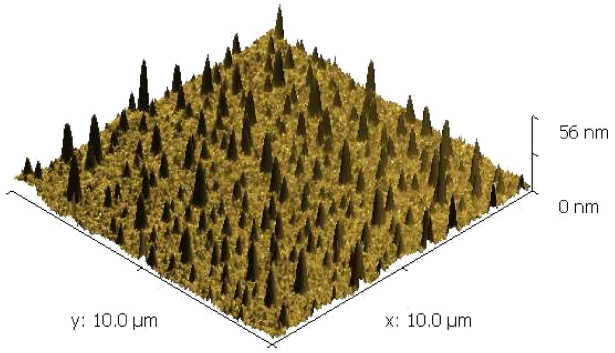

100 nm WO_3, 30°C, p-p 67 nm

Fig. 9. Morphology of the surface of the WO_3 layer deposited on the substrate at a temperature of 30°C

Catalytic Pd layers were obtained in the same process of evaporation (without opening the vacuum chamber) by vacuum evaporation of palladium (1 10^{-3} Pa) from a tungsten heater (wire diameter of 1 mm). The palladium deposition rate was 0.3 nm/sec. A view of a multi-channel SAW sensor is to be seen in Fig. 10.

The cycles of investigations comprised subsequent stages of filling the measurement chamber with a volume about 0.3 cm^3 (jointly with the installation supplying the methane from the mixer amounted – about 2 cm^3) with a methane concentration of 500 to 125 ppm in synthetic air and dry synthetic air. Each cycle lasted 2×600 seconds. These investigations were carried out at a temperature of the sensor amounting to 80°C and 100°C. The results concerning two WO_3 layers with a thickness of 50 nm and 100 nm have been presented in Fig. 11. The response obtained in the layer with the thickness of 150 nm was only slight and has been neglected in the graph. The duration of responses resulting from the diagram and the time of regeneration of the sensor layers amounted, respectively, to 60 and 100 seconds. Numerical analysis shows that the reaction layer of the sensor is fast, so that the sensor response time is mainly due to time needed for the filling the installation (chamber and pipe) with gas and to establish the composition of the mixture. The results of the investigations prove the existence of an optimal thickness of the sensor layer maximizing the responses (in the case of the presented experiment the highest response is achieved in a layer with the thickness of 50 nm – about 6 kHz at 500 ppm CH_4 (Fig. 13). Numerical investigations (Figs. 7c and 8c) indicate that the optimal thickness of the layer is about 40 nm.

a)

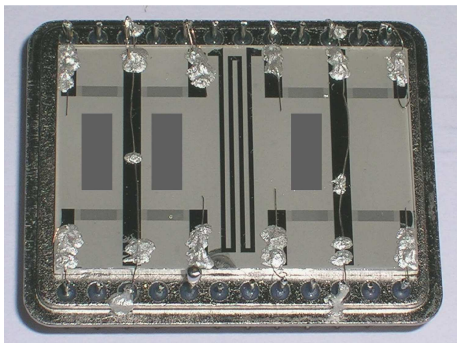

b)

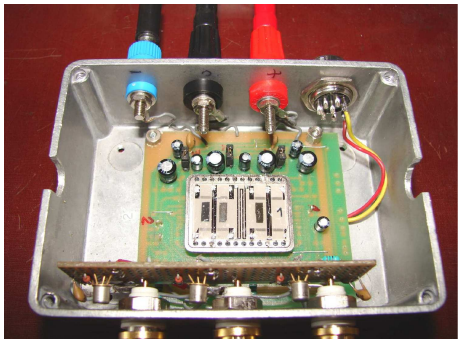

Fig. 10. The system of 4 acoustic lines on the $LiNbO_3$ substrate with 3 sensors layers and a reference line

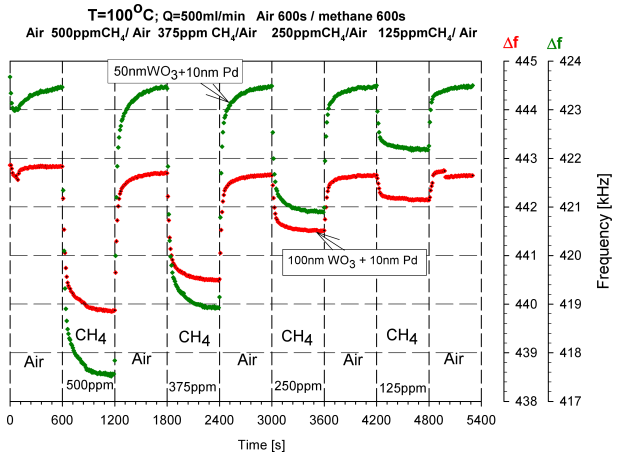

Fig. 11. Response of SAW sensor Δf with a WO_3 + Pd layer, 50 and 100 nm thick, to with concentrations of 500 to 125 ppm in air. Temperature of the sensor was 100°C

An increase of the working temperature of the sensors from 80 to 100°C causes increased responses of the sensors

(Fig. 12). The results of experiment coincide with the results of analyses presented in Fig. 7d.

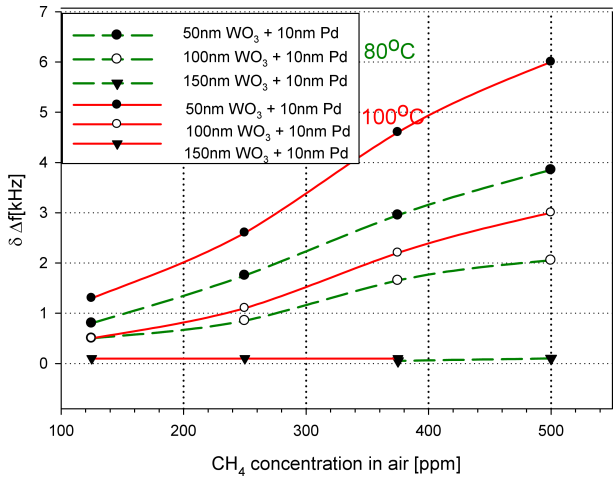

Fig. 12. Changes of the differentia frequency $\delta\Delta f$ in the SAW sensor vs. concentration of the methane in air at temperature 80°C and 100°C of a sensor with WO_3 + Pd layers (thickness of WO_3: 50, 100 and 150 nm)

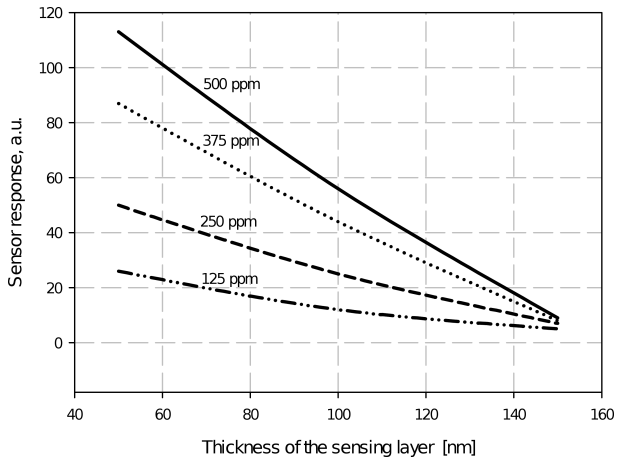

Fig. 13. SAW sensor response to methane (500, 375, 250 and 125 ppm) vs. thickness of the sensor layer (WO_3) at 100 °C

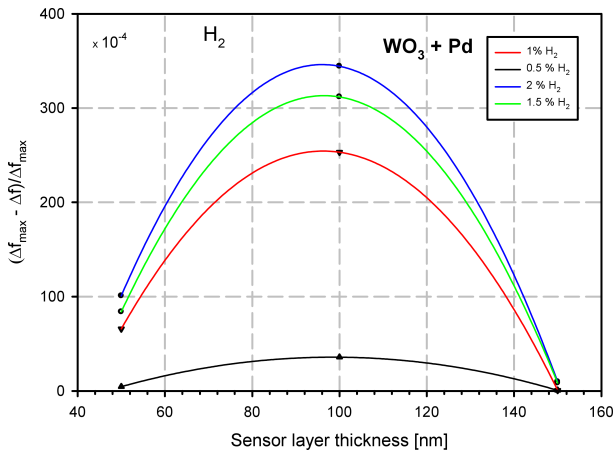

Fig. 14. Experimental results for WO_3 + Pd sensor layers at thickness 50 nm, 100 nm and 150 nm at various concentrations of H_2 gas after Ref. [15]. Optimal sensor layer thickness is about 90 nm

The optimum thickness of the sensor layer depends on the porosity of the layer and the type (size) of gas molecules. In the studies presented in [15] concerning hydrogen the optimal thickness of the WO_3 sensor layer was approximately 90 nm. A hydrogen molecule is much smaller than a molecule of methane (molar mass are respectively 2 and 16 g/mol), so its diffusion to the sensor layer is different. Thus, the concentration profile of the gas molecules and the electric charge in the sensor layer differ.

5. Summary

Basing on the mechanism of Knudsen's diffusion of gas molecules in a porous sensor layer, the profiles of the concentration of gas molecules in a steady-state layer was determined, concerning methane, ethane, propane, benzene (CH_4,C_2H_4, C_3H_8, C_6H_6), and in the non-steady state concerning the methane CH_4. Thus, changes in the velocity of an elastic wave in the sensor structure could be determined. These changes are correlated with the response of the sensor. The numerical calculations concerned a semiconductor layer of WO_3 (E_g = 2.7 eV). The results of the numerical analysis of the effect of such factors as the concentration of gas molecules in the environment, the thickness and porosity of the sensor layer and the temperature of the sensor, on changes of the velocity of propagation of Rayleigh's wave have been presented. The optimal thickness of the sensor layer depends on the porosity of the layer and the size of gas molecules. It may be said that practically analyzed system in the steady state sets in after a few milliseconds. The results of numerical analyses have been verified by experimental investigations. Experimental studies have confirmed the usefulness of the analytical model for designing the parameters of the SAW sensor.

Acknowledgements. The work is financed by the NCBR within the grant No: OR00017912.

REFERENCES

[1] E. Maciak and Z. Opilski, "Transition metal oxides covered Pd film for optical H_2 gas detection", *Thin Solid Films* 515, 8351–8355 (2007).

[2] T. Pustelny, J. Ignac-Nowicka, and Z. Opilski, "Optical investigations on layered metalphthalocyanine nanostructures affected by NO_2 applying the surface plasmon resonance method", *Optica Applicata* 34 (4), 563–572 (2004).

[3] W. Jakubik, M. Urbańczyk, E. Maciak, and T. Pustelny, "Surface acoustic wave hydrogen sensor based on layered structure of palladium/metal – free phthalocyanine", *Bull. Pol. Ac.: Tech.* 56 (2), 133–138 (2011).

[4] M. Urbańczyk , E. Maciak, K. Gut, T. Pustelny, and W. Jakubik, "Layered thin film nanostructures of Pd /WO3-x as resistance gas sensors", *Bull. Pol. Ac.: Tech.* 59 (4), 401–408 (2011).

[5] T. Hejczyk, M. Urbańczyk, and W. Jakubik, "Analytical model of semiconductor sensor layers in SAW gas sensors", *Acta Physica Polonica* A 118 (6), 1148–1152 (2010).

[6] T. Hejczyk and M. Urbańczyk, "Analysis of non-steady state in SAW gas sensors with semiconducting sensor layers", *Acta Physica Polonica* A 120 (4), 789–793 (2011).

[7] T. Hejczyk, M. Urbańczyk, and W. Jakubik, "Semiconductor sensor layer in SAW gas sensors configuration", *Acta Physica Polonica* A 118 (6), 1153–1157 (2010).

[8] M.Urbańczyk, *Gas Sensors with Surface Acoustic wave*, Publishing House of Silesian University of Technology, Gliwice, 2011, (in Polish).

[9] M. Urbańczyk "Analytical model of a SAW gas sensor*", WIT Trans. on Computational Methods and Experimental Measurements, Proc. CMEM11* 48, 229–239 (2011).

[10] G.S. Kino, "A normal mode theory for the Rayleigh wave amplifier", *IEEE Trans. on Electron Devices* Ed-18 (10), CD-ROM (1971).

[11] B.A. Auld, *Acoustic Fields and Waves*, vol. 2, John Willey and Sons, New York, 1973.

[12] J. Crank*, The Mathematics of Diffusion*, Oxford University Press, London, 1956.

[13] G. Sakai, N. Matsunaga, E.Shimanoe, and N. Yamazone, "Theory of gas-diffusion controlled sensitivity for thin film semiconductor gas sensor", *Sensors and Actuators* B 80, 125–131 (2001).

[14] N. Matsunga, G. Sakai, K. Shimanoe, and N. Yamazoe, "Diffusion equation-based study of thin film semiconductor gas sensor-response transient", *Sensors and Actuators* B 83, 216–221 (2001).

[15] T. Hejczyk and M. Urbańczyk, "WO_3-Pd structure in SAW sensor for hydrogen detection", *Acta Physica Polonica* A 120 (4), 616–620 (2011).